**Neuron, Volume *99***

## Supplemental Information

# miRNA-711 Binds and Activates TRPA1 Extracellularly to Evoke Acute and Chronic Pruritus

**Qingjian Han, Di Liu, Marino Convertino, Zilong Wang, Changyu Jiang, Yong Ho Kim, Xin Luo, Xin Zhang, Andrea Nackley, Nikolay V. Dokholyan, and Ru-Rong Ji**

**Supplemental Information**

# miRNA-711 binds and activates TRPA1 extracellularly to evoke acute and chronic pruritus

Qingjian Han, Di Liu, Marino Convertino, Zilong Wang, Changyu Jiang, Yong Ho Kim, Xin Luo, Xin Zhang, Andrea Nackley, Nikolay V Dokholyan, & Ru-Rong Ji

## Supplemental Figures

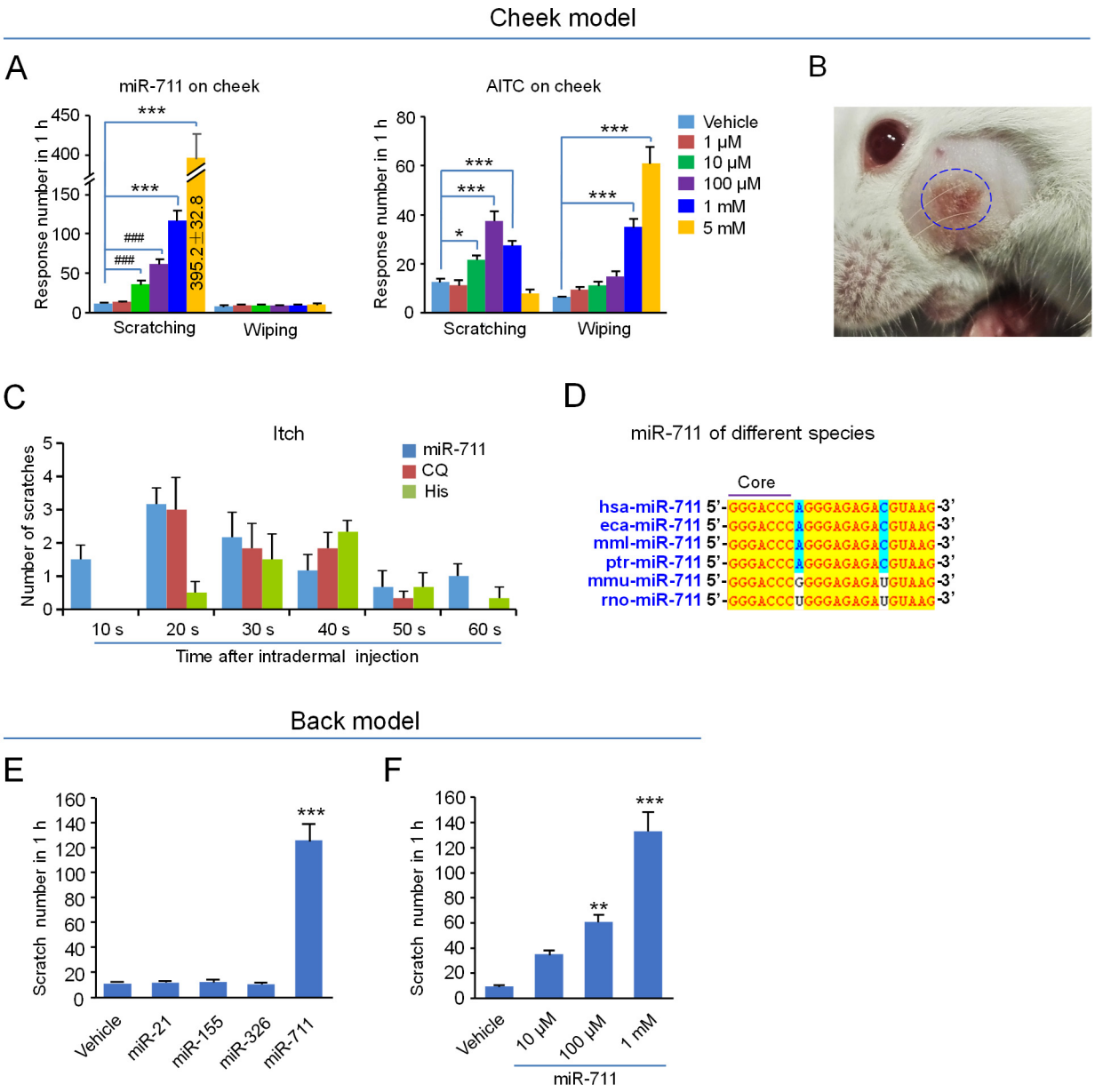


**Figure S1 (Related to Figure 1).** Characterization of miR-711-induced itch in the cheek model in mice.

**(A)** Intradermal injection of miR-711 induces dose-dependent scratching, but intradermal AITC evokes both pain and itch. ***$P$<0.001, vs. vehicle, One-Way ANOVA, n = 6 mice/group. ###$P$<0.001 vs. vehicle, Two-tailed Student's t-test, n = 6 mice/group. Note that miR-711 fails to induce wiping at all the concentrations. In contrast, intradermal AITC induces scratching at low concentrations but wiping at high concentrations. *$P$<0.05, ***$P$<0.001, vs. vehicle, One-Way ANOVA, n = 7 mice/group.

**(B)** Intradermal miRNA-711 at the highest concentration (5 mM) causes skin lesion on the cheek, as indicated by blue circle, 1 h after intradermal injection.

**(C)** Analysis of acute itch within the first 60 sec following intradermal cheek injection of miR-711 (1 mM, 10 μl), chloroquine (CQ, 100 μg in 10 μl), and histamine (200 μg in 10 μl). Note a faster induction of scratching by miR-711 within first 10 sec after the injection. n = 6 mice/group.
**(D)** Sequence alignment of miR-711 in different species. Note that the GGGACCC core sequence is identical in all the species.
**(E,F)** Intradermal miR-711 also evokes marked pruritus on the back of mice.
**(E)** Intradermal nape injection of mmu-miR-711, but not mmu-miR-21, mmu-miR-155, or mmu-miR-326 at 1 mM (10 μl), induces scratching. ***$P$<0.001, vs. vehicle, One-Way ANOVA, n = 6 mice/group.
**(F)** Intradermal nape injection of miR-711 induces dose-dependent scratching. **$P$<0.01, ***$P$<0.001, vs. vehicle, One-Way ANOVA, n = 6 mice/group.
Data are Mean ± SEM.

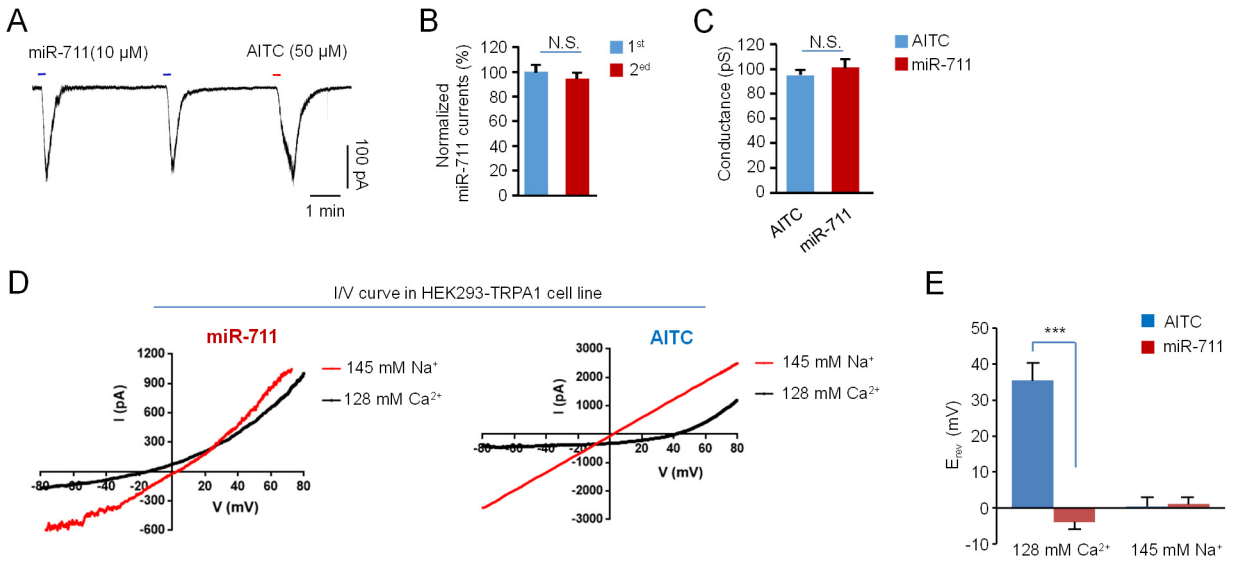


**Figure S2 (Related to Figure 2).** Additional characterization of TRPA1 activation by miR-711 and AITC in HEK293 cells expressing hTRPA1.

**(A, B)** miR-711(10 μM) does not cause TRPA1 desensitization after the 2nd application.

**(A)** Traces of inward currents.

**(B)** Quantification of inward current induced by first and second application of miR-711 (10 μM). N.S., not significant, Two-tailed Student's t-test, n = 10 cells/group.

**(C)** Single channel conductance of hTRPA1 activated by mmu-miR-711 and AITC in HEK293 cells expressing hTRPA1. Related to outside-out recordings in Figures 2H, 2I. N.S., not significant, Two-tailed Student's t-test, n = 5 cells/group.

**(D)** I/V analysis shows different permeability to calcium and sodium in *Trpa1*-expressing HEK293 cells in response to miR-711 (10 μM) and AITC (50 μM).

**(E)** Quantification of reverse potential to $Ca^{2+}$ and $Na^{+}$, ***$P$<0.001, Two-tailed Student's t-test, n = 5-10 cells per group. Note that AITC and miR-711 cause distinctive permeability changes in $Ca^{2+}$ and $Na^{+}$.

Data are Mean ± SEM.

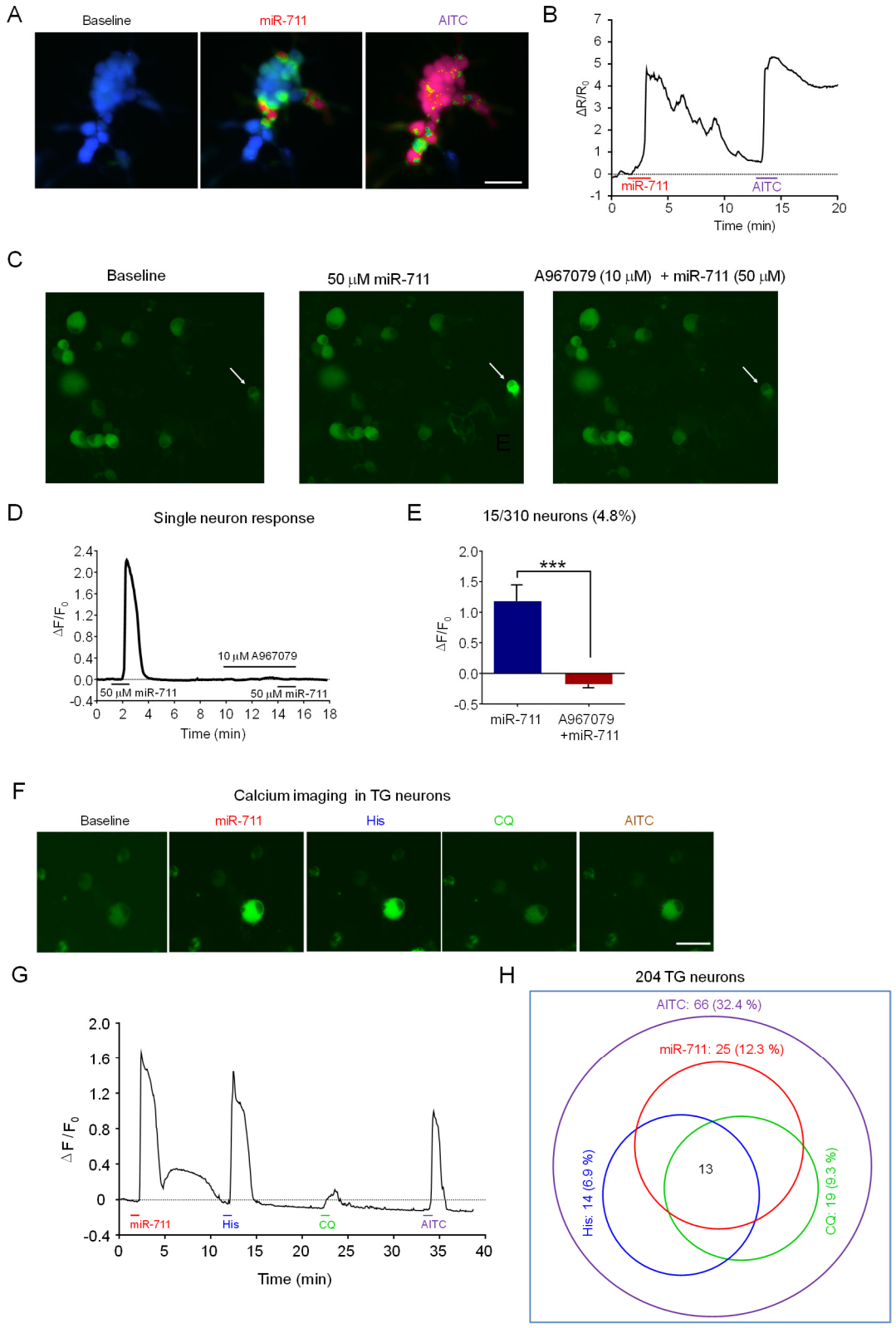


**Figure S3 (Related to Figure 3).** miR-711 induces calcium responses in hTRPA1-expressing HEK293 cells and dissociated DRG and trigeminal ganglion (TG) neurons of Pirt-GCaMP3 mice.

**(A)** Representative images of calcium changes in HEK293 cells in response to mmu-miR-711 (50 μM) and AITC (50 μM). Cells were incubated with 2 μM Fura-2 for 40 min. Scale is 50 μm.
**(B)** Typical calcium traces show a HEK293 cell response to miR-711 and AITC.
**(C-E)** miR-711 (50 μM) evoked calcium responses in mouse DRG neurons of Pirt-GCaMP3 mice before and after the treatment of TRPA1 antagonist A967079 (10 μM).
**(C)** Representative images of DRG neurons. Scale is 50 μm.
**(D)** Typical calcium trace of a mouse neuron.
**(E)** Quantification of calcium response. Note 15 of 310 (4.8%) neurons showed calcium responses to miR-711, which is completely blocked by A967079. **P*<0.001, t-test, n=15.
**(F-H)** Calcium responses in TG neurons of Pirt-GCaMP3 mice.
**(F)** Representative images of TG neurons in response to mmu-miR-711 (50 μM), histamine (His, 500 μM), chloroquine (CQ, 1000 μM), and AITC (200 μM). Scale is 50 μm.
**(G)** Typical calcium traces of a TG neuron in response to mmu-miR-711, Histamine, CQ, and AITC.
**(H)** Venn diagram showing overlaps between miR-711-responvie neurons and histamine, CQ, and AITC responsive neurons and the percentage of each population in TG neurons. A total of 204 neurons from 3 mice were analyzed, and 13 TG neurons respond to all the stimuli.

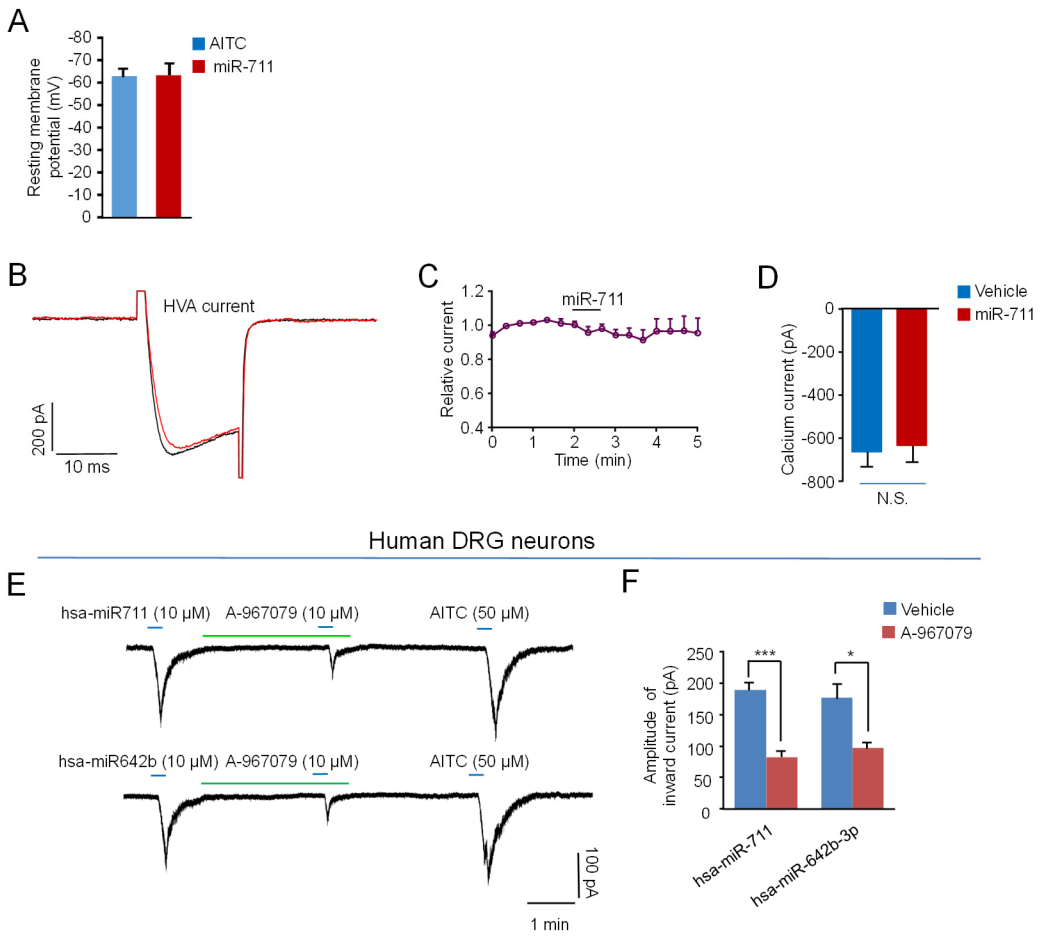


**Figure S4 (Related to Figure 4).** Action potentials, calcium currents, and resting membrane potentials of mouse DRG neurons and inward currents in human DRG neurons following miR-711 treatment.

**(A)** The resting membrane potentials (RMPs) of DRG neurons prior to the treatment of miR-711 (10 μM) and AITC (50 μM). n = 7-9 neurons per group. Notice all DRG neurons have similar RMPs before the treatment.

**(B-D)** miR-711 (10 μM) does not inhibit calcium currents in dissociated small-diameter mouse DRG neurons.

**(B)** Trace of calcium currents before and after mmu-miR-711 (10 μM) treatment.

**(C)** Time-course of relative calcium currents. DRG neurons were treated with miR-711 (10 μM) for 1 min, n = 6 neurons.

**(D)** Quantification of calcium currents before and after miR-711 perfusion. N.S., not significant, Two-tailed Student's t-test, n = 6 neurons.

**(E, F)** Inward currents evoked by miRNAs and AITC in dissociated human DRG neurons with small diameters (< 50 μm).

**(E)** hsa-miR-711 and hsa-miR-642b (10 μM) evoke TRPA1-dependent inward currents in human DRG neurons. Note the currents were blocked by A967079 (10 μM).

**(F)** Quantification of inward currents in human DRG neurons. **P*<0.05, ****P*<0.001, Two-tailed Student's t-test, n = 4 neurons per group from 4 donors.

Data are Mean ± SEM.

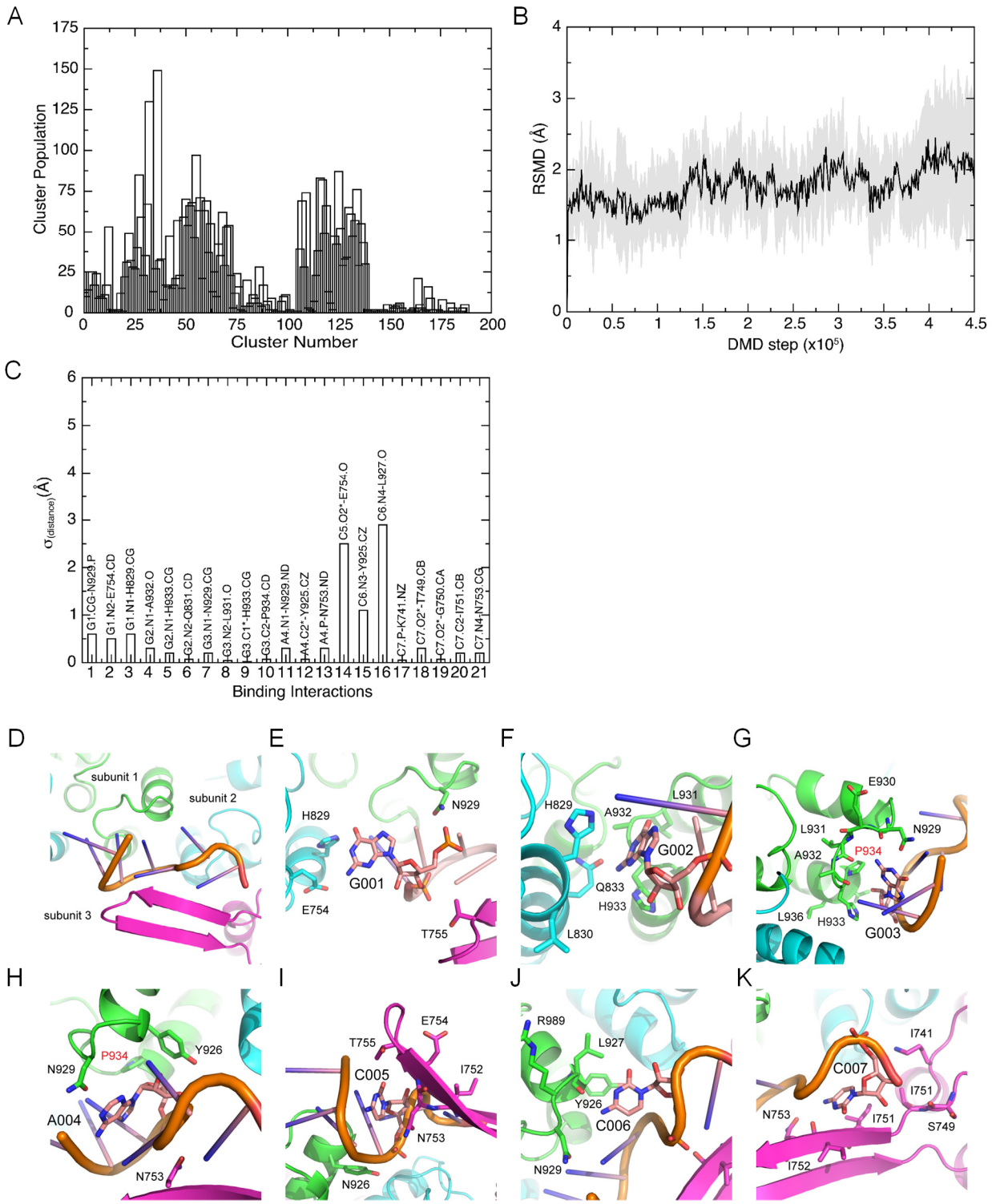


**Figure S5 (Related to Figure 5).** Computer simulations show the interactions between hTRPA1 and the core sequence of miR-711.

**(A)** Cluster population of high affinity GGGACCC/TRPA1 conformations. The ensemble of high affinity GGGACCC/TRPA1 conformations (*i.e.*, binding energy lower or equal to -75 kcal/mol) were clustered according to the RSMD computed over the GGGACCC phosphorus atoms, using

a cutoff of 4.24 Å to distinguish two distinct conformations. The conformations of the most populated clusters (~ 4% of the isolated conformational space) were used to explore the binding mode of GGGACCC to hTRPA1 and the lowest binding energy conformation of the ensemble (*i.e.*, -87 kcal/mol) is chosen as the representative structure of miRNA-711-TRPA1 complex.
**(B)** Fluctuation of TRPA1-bound GGGACCC conformation. The average RMSD (in black) and standard deviation (grey) of GGGACCC phosphorus atoms is computed over five independent, $4.5x10^5$ step-long DMD simulations at temperature 0.3 kcal/(mol $k_B$).
**(C)** Fluctuations of inter-atomic distances between GGGACCC and TRPA1. Standard deviation of distances between atoms of GGGACCC and TRPA1 residues interacting within 5 Å of each nucleobase are computed over five independent, $4.5x10^5$ step-long DMD simulations at temperature 0.3 kcal/(mol $k_B$).
**(D-K)** Detailed views of the binding interactions between each nucleotide of the GGGACCC core sequence and hTRPA1, including G001 (E), G002 (F), G003 (G), A004 (H), C005 (I), C006 (J), and C007 (K), with special focus on P937 with G003 and A004 within 5 Å. P937 is highlighted in red.

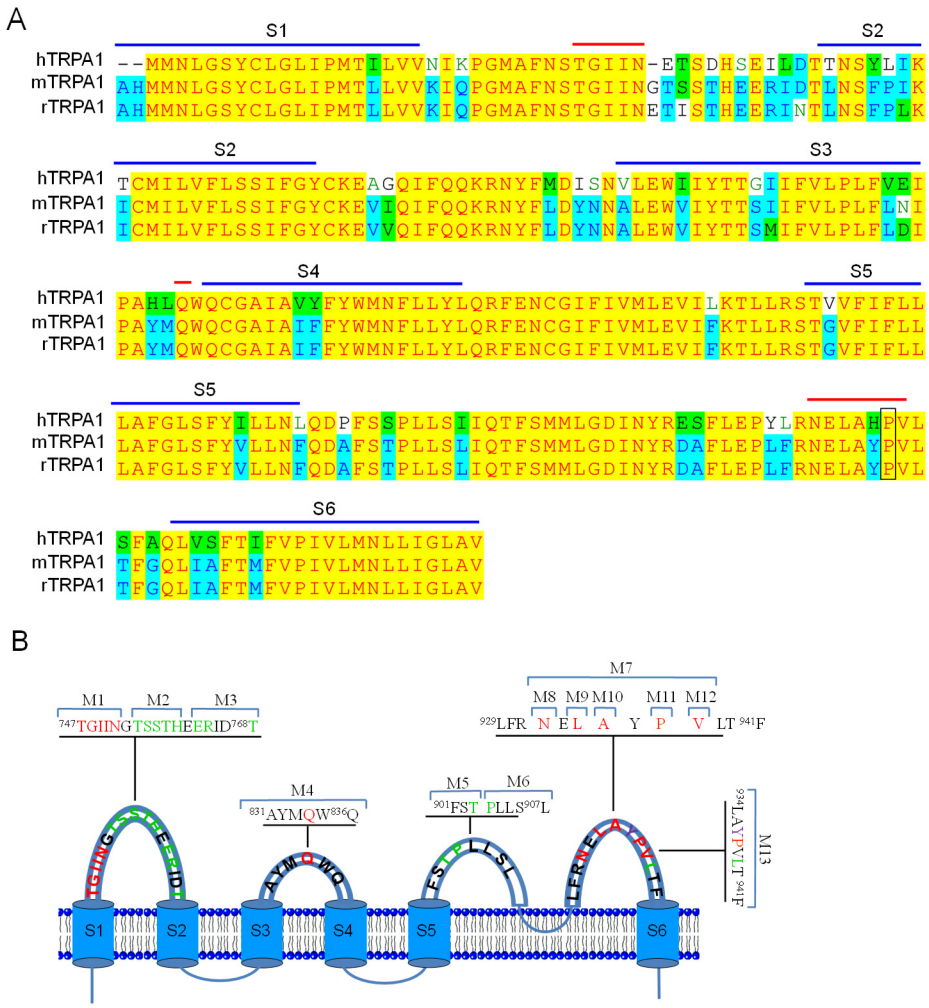


| Location | mTRPA1 mutants | Mutated residues on mTRPA1 | % inhibitiorn of AITC current | % inhibition of miR-711 current |
|---|---|---|---|---|
| Extracellular loop 1 | M1 | $T^{751A}G^{752A}I^{753A}I^{754A}N^{755A}$ | 54.2 | 57.6 |
| | M2 | $T^{757A}S^{758A}S^{759A}T^{760A}H^{761A}$ | 12.5 | 5.7 |
| | M3 | $E^{763A}R^{764A}IDT^{767A}$ | 5.4 | 4.0 |
| Extracellular loop 2 | M4 | $Q^{844A}$ | 3.4 | 10.4 |
| Extracellular loop 3 | M5 | $T^{903A}$ | 2.1 | 14.4 |
| | M6 | $P^{904A}$ | 82.2 | 80.2 |
| | M7 | $N^{932A}EL^{934A}A^{935D}YP^{937A}V^{938A}$ | 61.9 | 74.4 |
| | M8 | $N^{932A}$ | 40.5 | 59.1 |
| | M9 | $L^{934A}$ | 92.9 | 93.6 |
| | M10 | $A^{935D}$ | 16.0 | 20.8 |
| | M11 | $P^{937A}$ | **3.8** | **53.7** |
| | M12 | $V^{938A}$ | 99.5 | 98.4 |
| | M13 | $Y^{935A}P^{937A}VL^{939A}$ | **14.9** | **84.8** |

**Figure S6 (Related to Figure 6).** Alignment of TRPA1 sequences of different species and effects of mTRPA1 mutations on inward currents induced by ATIC and miR-711 in CHO cells

**(A)** Amino acids sequence alignment of human, mouse, and rat TRPA1. S1-S6 are six transmembrane segments indicated by blue lines. Predicated residues with possible interactions with miR-711 core sequence are shown with red lines. Ultra-conservative amino acids among all

three species are highlighted in yellow. Blue box indicates the residue P934 of hTRPA1, which is equivalent to P937 of mTRPA1.
**(B, C)** Effects of mTRPA1 mutations on AITC- or miR-711-induced inward current in CHO cells transfected with wild type or mutant *Trpa1* cDNAs.
**(B)** Schematic of mTRPA1 domains on cell membrane. Predicted and ultra-conservative amino acids were highlighted in red, predicted but non-conservative amino acids were labeled in purple, and randomly selected and non-predicted amino acids were labeled in green. Black residues are non-mutated ones. A total of 13 mutants in extracellular loop 1-3 were generated as indicated.
**(C)** Summary of different mutants of mTRPA1 and their effects (% inhibition) on AITC (50 μM) or miR-711 (10 μM) induced inward currents in CHO cells transfected with wild type or mutated *Trpa1* cDNAs. Red residues are conservative ones predicted by computer simulation, and green residues were randomly selected on extracellular loops. Purple residues are non-conservative sites predicted by computer simulation. Specific mutations (M11 and M13) that only cause reduction in miR-711 but not AITC currents (bold in black) are underlined. n = 6-15 cells per condition.

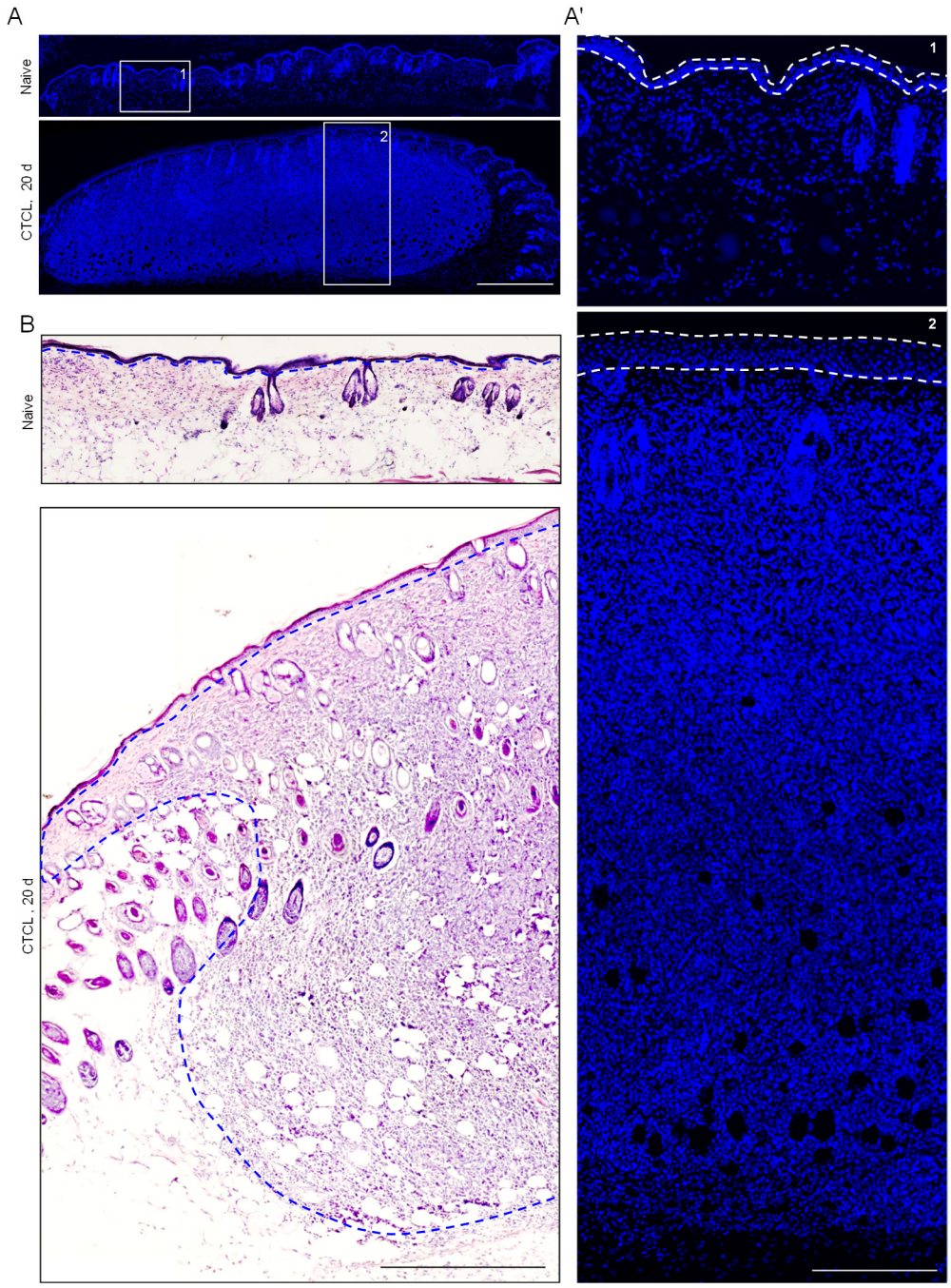


**Figure S7 (Related to Figure 7).** Characterization of lymphomas on the back skin of CTCL mice
(A) Images of DAPI staining of normal and tumor-bearing skins after CTCL. Scale, 1 mm.
**(A')** Enlarged box-1 and box-2 in A. Scale, 250 μm.
**(B)** Images of HE staining of normal and tumor-bearing skins after CTCL. Scale, 500 μm. Dashed lines indicate the epidermis.

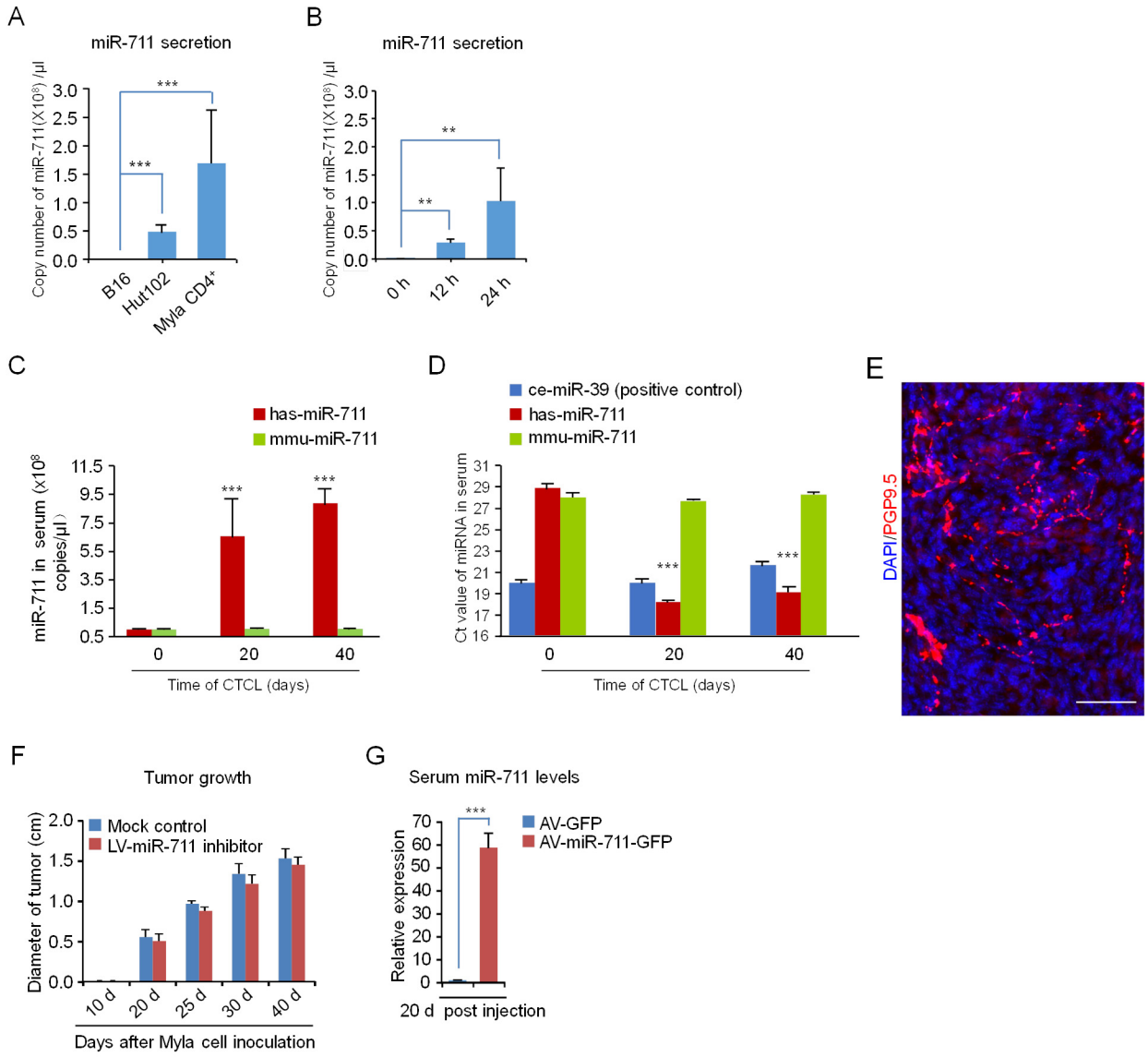


**Figure S8 (Related to Figure 7 and Figure 8).** Characterization of miR-711 secretion in culture media and mouse serum and nerve innervation and tumor growth in the CTCL model.

**(A)** hsa-miR-711 secretion in tumor cell cultures. A total of 1 million B16 cells, HuT102 cells, and CD4$^+$ Myla cells were plated into 2 ml culture medium, and 0.2 ml of medium were collected 24 h after subculture for qRT-PCR analysis. Note that melanoma B16 cells do not secrete hsa-miR-711. ***$P$<0.001, vs. B16, One-Way ANOVA, n = 3 replications/group.

**(B)** Time course of hsa-miR-711 secretion in culture media. One million CD4$^+$ Myla cells were plated into 2 ml culture medium, 0.2 ml medium was collected at 0 h, 12 h and 24 h after subculture for qRT-PCR analysis. **$P$<0.001, vs. 0 h, One-Way ANOVA, n = 3 replications/group.

**(C, D)** Secretion of hsa-miR-711 and mmu-miR-711 in serum of control and CTCL mice.

**(C)** Copy number of hsa-miR-711 and mmu-miR-711 in serum of naïve, CTCL 20 d, and CTCL 40 d mice.

**(D)** Ct values of miRNA levels shown in (C).

**(E)** Nerve innervation, as revealed by PGP 9.5 immunostaining, in the skin lymphoma 20 days after Myla cell inoculation. DAPI staining shows all the nuclei of the tumor cells. Scale, 100 µm.
**(F,G)** Tumor growth and miR-711 secretion after lentivirus (LV) over-expression of miR-711 inhibitor in Myla cells before the inoculation.
**(F)** miR-711 inhibitor does not affect the tumor growth. Two-Way ANOVA, n = 7 mice/group.
**(G)** Relative serum expression levels of miR-711 10 days after nape injection of AV-GFP (Mock control) and AV-miR-711-GFP (10 µl, titer of $2x10^{11}$ GC/ml). ***$P<0.001$ vs. AV-GFP control, Two-tailed Student's t test, n = 3-4 mice/group.
Data are Mean ± SEM.